Acta Mech 226, 643–664 (2015)
DOI 10.1007/s00707-014-1219-9

Vlado A. Lubarda

Circular inclusion near a circular void: determination of elastic antiplane shear fields and configurational forces

Received: 24 April 2014 / Published online: 26 July 2014

Abstract The stress and displacement fields are determined inside and outside a circular inclusion located in the vicinity of a circular void in an infinite elastic solid, within a circular cylinder, or near the free surface of a half-space, in the case when the inclusion is characterized by a uniform eigenstrain of the antiplane shear type. The fields are obtained as the sum of their infinite-medium stress fields and the calculated auxiliary fields. It is shown that the fields outside the inclusion follow directly from the extended Milne-Thomson circle theorem, but not the fields inside the inclusion. The overall fields are interpreted as the superposition of the infinite-medium fields from the actual and the image inclusion of the appropriate location, radius, and eigenstrains. The stress amplification is evaluated for the inclusion approaching the boundary of the void, cylinder, or half-space. The configurational forces are then evaluated, associated with a relative translation of the void and inclusion, or the expansion of the void or inclusion. The J and M integrals along the boundary of the void are evaluated without using the solution of the entire boundary-value problem, but only the stress field for an inclusion in an unvoided infinite medium. This is accomplished by incorporating the result that the circumferential shear stress along the boundary of a traction-free circular void in an infinite isotropic solid under antiplane shear is twice the circumferential shear stress along the corresponding circle in an infinite solid without a void, under the same loading conditions. The energy release rate associated with a self-similar expansion of the inclusion is calculated from the determined elastic field around the inclusion and from the evaluated total strain energy of the system. The configurational forces on the inclusion in a circular cylinder and near the free surface of a half-space are also determined and discussed.

1 Introduction

This paper is devoted to the analysis of elastic fields around a circular inclusion in the vicinity of a circular void in an infinite isotropic solid, inside a circular cylinder, and near the free surface of a half-space, under antiplane strain conditions. The analysis is of interest for the study of displacive/martensitic and stress-induced phase transformations, twinning in ceramic and crystalline materials, interactions between precipitates and voids, and the analysis of piezoelectric fibers embedded in a matrix material. Previously, the antiplane eigenstrain problem of a circular or ellipsoidal inclusion was addressed mostly for the inclusion in an infinite or semi-infinite

Dedicated to the memory of Professor George Herrmann.

V. A. Lubarda (✉)
Departments of NanoEngineering and Mechanical and Aerospace Engineering, University of California,
San Diego, La Jolla, CA 92093-0448, USA
Tel.: 858-534-3169
E-mail: vlubarda@ucsd.edu

V. A. Lubarda
Montenegrin Academy of Sciences and Arts, Rista Stijovića 5, 81000 Podgorica, Montenegro

medium, albeit with the included elastic anisotropy [1–4], or with the more involved material models, such as those of nonlocal elasticity [5], couple-stress elasticity [6,7], piezoelectric materials [8–10], functionally graded materials [11], or nonlinear elasticity [12]. A related problem, of interest for the mechanics of composite materials, is the problem of a circular inhomogeneity near a void or another inhomogeneity, under remote loading. This was analyzed in great detail in [13,14] by the procedure referred to as heterogenization. Circular inclusions with imperfect interfaces were considered in [15,16]. The evaluation of the stress and displacement fields due to internal sources of stress is of great importance for the study of various problems in materials science [17–20]. For example, the evaluation of the attraction exerted on the dislocation by the free surface of void plays a prominent role in the study of a void growth by dislocation emission [21–25]. The interaction between a screw dislocation and an elliptical inclusion was considered in [26]. A curved mode III crack in a circular cylinder or near the free surface of a half-space was studied in [27]. A comprehensive review of recent works on inclusions can be found in [28].

In the present paper, we derive the stress and displacement fields in an infinite isotropic elastic solid weakened by a circular cylindrical void, due to a nearby circular inclusion characterized by uniform eigenstrain of the antiplane shear type. The fields are obtained as the sum of their infinite-medium stress fields and the calculated auxiliary fields. The fields outside the inclusion follow directly from the extended Milne–Thomson circle theorem [29–32], but not the fields inside the inclusion. It is shown that the overall fields represent the superposition of the infinite-medium fields of the actual and the image inclusion having appropriately specified location, radius, and eigenstrains. The obtained results complement classical results for a screw dislocation and a concentrated line force near the free surface of a void or a half-space [33–35]. The analysis also delivers the results for the inclusion within a circular cylinder and near the free surface of a half-space. The stress amplification is evaluated for the inclusion approaching and, in the limiting case, becoming tangent to the boundary of the void, cylinder, or half-space.

The second objective of the paper is the determination of the configurational forces acting on the void or inclusion in the framework of configurational mechanics. The evaluation of material forces on defects by using the J and M conservation integrals is particularly effective in cases when they can be evaluated without solving the entire boundary-value problem under consideration. A number of such cases were considered in the past, such as the evaluation of the energy release rate for an edge crack or the plane version of conical crack [36], semi-infinite and finite crack under concentrated load, ligament between two semi-infinite cracks, or a wedged open crack [37], and the attraction of a dislocation to a notch tip and bicrystal interface [38]. The configurational force between an edge dislocation and circular void by evaluating the J and M integrals around the boundary of the void was determined in [39], and on a screw dislocation near a circular elastic inhomogeneity in [40]. The expression for the configurational force between two inhomogeneities in an infinite matrix under remote loading was derived in [41]. In the present paper, we determine the configurational force exerted by the free surface of a circular void on a circular inclusion with uniform eigenstrain. The configurational force is calculated by evaluating the J integral along the boundary of the void, without resource to the solution of the entire boundary-value problem. This is accomplished by using the result from [32] that the circumferential shear stress along the boundary of a circular void in an infinite isotropic elastic solid under antiplane shear is twice the circumferential shear stress along the corresponding circle in an infinite solid without a void, under the same loading conditions. It is shown that this force depends on the magnitude of total eigenstrain, but not on the ratio of the eigenstrain components. The M integrals around the void and inclusion are also evaluated by using only the infinite-medium stress field. The energy release rate associated with a uniform expansion of the inclusion is then calculated and related to the M integral around the inclusion, which differs from this energy rate. The configurational forces on the inclusion in a circular cylinder and near the free surface of a half-space are lastly determined.

2 Circular inclusion near a void

Consider a circular cylindrical void of radius a in an infinitely extended isotropic elastic solid, and a circular cylindrical inclusion with its center at point C, at distance d from the center O of the void, Fig. 1a. The radius of the inclusion is $b \leq (d - a)$, so that the entire inclusion is outside the void. The bonding between the inclusion and the surroundings is assumed to be perfect. The prescribed uniform eigenstrain in the inclusion is of the antiplane shear type, with the components $(\epsilon^{\bullet}_{zx}, \epsilon^{\bullet}_{zy})$. The corresponding out-of-plane displacement is $w^{\bullet} = 2\rho(\epsilon^{\bullet}_{zx}\cos\varphi + \epsilon^{\bullet}_{zy}\sin\varphi)$, where (ρ, φ) are the polar coordinates with respect to the center C of the inclusion. When the inclusion is inserted into the solid nearby the void, the stress field around the void can

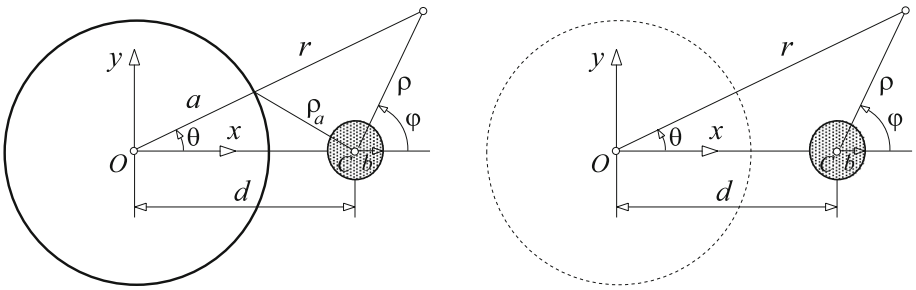

Fig. 1 **a** Circular inclusion of radius b in an infinite medium near the void of radius a. The eigenstrain of the inclusion is $(\epsilon^{\bullet}_{zx}, \epsilon^{\bullet}_{zy})$. The centers of the inclusion and void are at distance d. The distance from C to an arbitrary point on the boundary of the void is ρ_a. **b** Inclusion in an infinite medium without the void. The *dashed-line circle* coincides with the boundary of the void in a voided infinite medium from part (**a**)

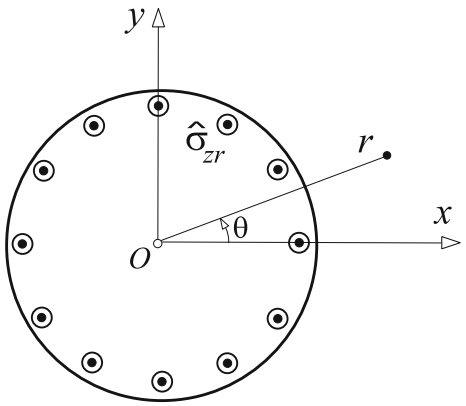

Fig. 2 The auxiliary problem in which the void in an infinite medium is loaded over its boundary $r = a$ with self-equilibrating traction $\hat{\sigma}_{zr}(a, \theta) = -\sigma^0_{zr}(a, \theta)$, where $\sigma^0_{zr}(a, \theta)$ is the radial shear stress component along the *circle* $r = a$ in an unvoided infinite medium from Fig. 1b

be determined by superposition. First, the stress distribution is found due to the inclusion in an infinite solid without the void (Fig. 1b). Denote the polar components of this stress field by $\sigma^0_{zr}(r, \theta)$ and $\sigma^0_{z\theta}(r, \theta)$, where (r, θ) are the polar coordinates with respect to the center of the void, as indicated in Fig. 1. Second, the auxiliary problem is solved for the void in an infinite medium, loaded on its surface $r = a$ by the self-equilibrating (image) traction $\hat{\sigma}_{zr}(a, \theta) = -\sigma^0_{zr}(a, \theta)$, as sketched in Fig. 2. The stress distribution of the original problem from Fig. 1a is the sum of the stress distributions for problems from Figs. 1b and 2, i.e.,

$$\sigma_{zr}(r, \theta) = \sigma^0_{zr}(r, \theta) + \hat{\sigma}_{zr}(r, \theta), \quad \sigma_{z\theta}(r, \theta) = \sigma^0_{z\theta}(r, \theta) + \hat{\sigma}_{z\theta}(r, \theta). \tag{1}$$

Likewise, for the displacement field,

$$w(r, \theta) = w^0(r, \theta) + \hat{w}(r, \theta). \tag{2}$$

2.1 Circular inclusion in an infinite medium

The stress field for a circular inclusion in an infinite solid is well known [34]. Expressed in polar coordinates (ρ, φ) with respect to the center of the inclusion (Fig. 1b), it can be written as

$$\begin{aligned} \sigma^{0,\text{in}}_{z\rho} &= -\mu\epsilon^{\bullet}_{z\rho}, & \sigma^{0,\text{in}}_{z\varphi} &= -\mu\epsilon^{\bullet}_{z\varphi}, \\ \sigma^{0,\text{out}}_{z\rho} &= -\mu(b^2/\rho^2)\epsilon^{\bullet}_{z\rho}, & \sigma^{0,\text{out}}_{z\varphi} &= \mu(b^2/\rho^2)\epsilon^{\bullet}_{z\varphi} \end{aligned} \tag{3}$$

where $\epsilon^{\bullet}_{z\rho} = \epsilon^{\bullet}_{zx}\cos\varphi + \epsilon^{\bullet}_{zy}\sin\varphi$ and $\epsilon^{\bullet}_{z\varphi} = \epsilon^{\bullet}_{zy}\cos\varphi - \epsilon^{\bullet}_{zx}\sin\varphi$. The shear modulus is μ, and the superscripts "in" and "out" designate the inside and outside inclusion fields. The displacements are

$$w^{0,\text{in}} = \rho\epsilon^{\bullet}_{z\rho}, \quad w^{0,\text{out}} = (b^2/\rho)\epsilon^{\bullet}_{z\rho}. \tag{4}$$

The rigid body displacement is chosen such that $w^{0,\text{in}} = 0$ at the center of the inclusion. The stress discontinuity across the boundary of the inclusion is $\Delta\sigma_{z\varphi}(b,\varphi) = -2\mu\epsilon^{\bullet}_{z\varphi}$.

When rewritten in terms of the polar coordinates (r,θ), the outside stress field takes the form

$$\begin{aligned}
\sigma^{0,\text{out}}_{zr}(r,\theta) &= -\frac{\mu b^2}{\rho^4}\left\{\left[(d^2+r^2)\cos\theta - 2dr\right]\epsilon^{\bullet}_{zx} - \left[(d^2-r^2)\sin\theta\right]\epsilon^{\bullet}_{zy}\right\},\\
\sigma^{0,\text{out}}_{z\theta}(r,\theta) &= \frac{\mu b^2}{\rho^4}\left\{\left[(d^2-r^2)\sin\theta\right]\epsilon^{\bullet}_{zx} + \left[(d^2+r^2)\cos\theta - 2dr\right]\epsilon^{\bullet}_{zy}\right\}
\end{aligned} \tag{5}$$

where

$$\rho^2 = d^2 - 2dr\cos\theta + r^2. \tag{6}$$

The corresponding displacement field is

$$w^{0,\text{out}}(r,\theta) = \frac{b^2}{\rho^2}\left[(r\cos\theta - d)\epsilon^{\bullet}_{zx} + (r\sin\theta)\epsilon^{\bullet}_{zy}\right]. \tag{7}$$

Along the circle $r = a$, the radial and circumferential shear stresses (omitting the superscript "out") are

$$\begin{aligned}
\sigma^{0}_{zr}(a,\theta) &= -\frac{\mu b^2}{\rho_a^4}\left\{\left[(d^2+a^2)\cos\theta - 2da\right]\epsilon^{\bullet}_{zx} - \left[(d^2-a^2)\sin\theta\right]\epsilon^{\bullet}_{zy}\right\},\\
\sigma^{0}_{z\theta}(a,\theta) &= \frac{\mu b^2}{\rho_a^4}\left\{\left[(d^2-a^2)\sin\theta\right]\epsilon^{\bullet}_{zx} + \left[(d^2+a^2)\cos\theta - 2da\right]\epsilon^{\bullet}_{zy}\right\}
\end{aligned} \tag{8}$$

in which $\rho_a^2 = d^2 - 2da\cos\theta + a^2$ is the square of the distance from the center of the inclusion to an arbitrary point on the boundary of the void.

The inside stress and displacement fields are

$$\begin{aligned}
\sigma^{0,\text{in}}_{zr} &= -\mu\epsilon^{\bullet}_{zr}, \quad \epsilon^{\bullet}_{zr} = \epsilon^{\bullet}_{zx}\cos\theta + \epsilon^{\bullet}_{zy}\sin\theta,\\
\sigma^{0,\text{in}}_{z\theta} &= -\mu\epsilon^{\bullet}_{z\theta}, \quad \epsilon^{\bullet}_{z\theta} = \epsilon^{\bullet}_{zy}\cos\theta - \epsilon^{\bullet}_{zx}\sin\theta,
\end{aligned} \tag{9}$$

and

$$w^{0,\text{in}}(r,\theta) = (r\cos\theta - d)\epsilon^{\bullet}_{zx} + (r\sin\theta)\epsilon^{\bullet}_{zy}. \tag{10}$$

The total strain energy (per unit thickness) is the sum of the strain energy inside and outside the inclusion. For inclusion in an infinite medium without void, this is

$$E^0_T = \frac{1}{2\mu}\left[\int_0^{2\pi}\int_0^{b}\left(\sigma^{0,\text{in}\ 2}_{z\rho} + \sigma^{0,\text{in}\ 2}_{z\varphi}\right)\rho\,\mathrm{d}\rho\,\mathrm{d}\varphi + \int_0^{2\pi}\int_b^{\infty}\left(\sigma^{0,\text{out}\ 2}_{z\rho} + \sigma^{0,\text{out}\ 2}_{z\varphi}\right)\rho\,\mathrm{d}\rho\,\mathrm{d}\varphi\right]. \tag{11}$$

Upon substitution of stress expressions and integration, it follows that the same amount of energy is stored within the inclusion as it is outside of it. The total energy is

$$E^0_T = \mu\left(\epsilon^{\bullet\ 2}_{zx} + \epsilon^{\bullet\ 2}_{zy}\right)b^2\pi. \tag{12}$$

2.2 Auxiliary fields

If $\sigma^0_{zr}(r,\theta)$ and $\sigma^0_{z\theta}(r,\theta)$ are stress components in the infinite medium outside the circle $r=a$ (Fig. 1b), the auxiliary stress components $\hat{\sigma}_{zr}(r,\theta)$ and $\hat{\sigma}_{z\theta}(r,\theta)$ for the problem in Fig. 2 can be determined from

$$\hat{\sigma}_{zr}(r,\theta) = -\frac{a^2}{r^2}\,\sigma^0_{zr}\left(a^2/r,\theta\right), \quad \hat{\sigma}_{z\theta}(r,\theta) = \frac{a^2}{r^2}\,\sigma^0_{z\theta}\left(a^2/r,\theta\right). \tag{13}$$

This follows from the circle theorem [29,30], extended to antiplane strain elasticity in [31] and [32]. By using the infinite-medium stress expressions (5), the auxiliary stress components (13) become

$$\begin{aligned}
\hat{\sigma}_{zr}(r,\theta) =& \frac{\mu b^2}{\hat{\rho}^4}\left\{\left[(a^2+d^2r^2/a^2)\cos\theta - 2dr\right]\epsilon^{\bullet}_{zx} + \left[(a^2-d^2r^2/a^2)\sin\theta\right]\epsilon^{\bullet}_{zy}\right\},\\
\hat{\sigma}_{z\theta}(r,\theta) =& \frac{\mu b^2}{\hat{\rho}^4}\left\{-\left[(a^2-d^2r^2/a^2)\sin\theta\right]\epsilon^{\bullet}_{zx} + \left[(a^2+d^2r^2/a^2)\cos\theta - 2dr\right]\epsilon^{\bullet}_{zy}\right\},
\end{aligned} \tag{14}$$

with

$$\hat{\rho}^2 = a^2 - 2dr\cos\theta + \frac{d^2}{a^2}\,r^2. \tag{15}$$

The corresponding displacement field is obtained from (7) by replacing there r with a^2/r and $\hat{\rho}^2$ with $(a^2/r^2)\hat{\rho}^2$. This gives

$$\hat{w}(r,\theta) = \frac{r^2b^2}{a^2\hat{\rho}^2}\left[\left(\frac{a^2}{r}\cos\theta - d\right)\epsilon^{\bullet}_{zx} + \left(\frac{a^2}{r}\sin\theta\right)\epsilon^{\bullet}_{zy}\right] + C_1 \tag{16}$$

where C_1 is an arbitrary constant. The auxiliary fields are derived by using the Fourier series method, without invoking the extended circle theorem, in "Appendix A".

3 Image inclusion

The auxiliary stress field (14) can be rewritten as

$$\begin{aligned}
\hat{\sigma}_{zr}(r,\theta) =& -\frac{\mu b_*^2}{\rho_*^4}\left\{\left[\left(d_*^2+r^2\right)\cos\theta - 2d_*r\right]\epsilon^*_{zx} - \left[\left(d_*^2-r^2\right)\sin\theta\right]\epsilon^*_{zy}\right\},\\
\hat{\sigma}_{z\theta}(r,\theta) =& \frac{\mu b_*^2}{\rho_*^4}\left\{\left[\left(d_*^2-r^2\right)\sin\theta\right]\epsilon^*_{zx} + \left[\left(d_*^2+r^2\right)\cos\theta - 2d_*r\right]\epsilon^*_{zy}\right\}
\end{aligned} \tag{17}$$

where

$$d_* = \frac{a^2}{d}, \quad b_* = \frac{a}{d}\,b, \quad \left(\epsilon^*_{zx},\epsilon^*_{zy}\right) = \left(-\epsilon^{\bullet}_{zx},\epsilon^{\bullet}_{zy}\right) \tag{18}$$

and

$$\rho_*^2 = d_*^2 - 2d_*r\cos\theta + r^2 = \frac{a^2}{d^2}\,\hat{\rho}^2. \tag{19}$$

The corresponding expression for the displacement is

$$\hat{w}(r,\theta) = \frac{b_*^2}{\rho_*^2}\left[(r\cos\theta - d_*)\epsilon^*_{zx} + (r\sin\theta)\epsilon^*_{zy}\right] + C_2 \tag{20}$$

where C_2 is an arbitrary constant, related to C_1 from (16) by $C_2 = C_1 - (b^2/d)\epsilon^{\bullet}_{zx}$.

If (20) is compared with (7), and (17) with (5), it is recognized that the stress and displacement fields of the auxiliary problem can be interpreted as the infinite-medium fields corresponding to an image inclusion of radius $b_* = (a/d)b$ and eigenstrain $(\epsilon^*_{zx},\epsilon^*_{zy}) = (-\epsilon^{\bullet}_{zx},\epsilon^{\bullet}_{zy})$, with its center placed at the distance $d_* = a^2/d$ from point O (Fig. 3). The radius of the image inclusion is constrained by the condition $b_* \le (a-d_*)$, because $d \ge (a+b)$. These results, not previously noted in the literature, complement the classical results for a screw dislocation near the free surface of a void or a half-space, where the opposite image dislocation is placed at the mirror position, and a concentrated line force near the free surface of a void or a half-space, where the image line force of the same sign (same direction as the actual force) is placed at the mirror position across the free surface [33–35,42,43].

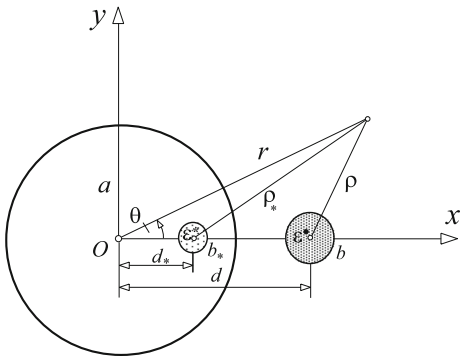

Fig. 3 A circular cylinder of radius a with the inserted inclusion of radius b and eigenstrains $(\epsilon^{\bullet}_{zx}, \epsilon^{\bullet}_{zy})$. The center of the image inclusion of radius $b_* = (a/d)b$ and eigenstrains $(-\epsilon^{\bullet}_{zx}, \epsilon^{\bullet}_{zy})$ is at the distance $d_* = a^2/d$ from the center of the cylinder, where d specifies the center of the actual inclusion. The radii r, ρ and ρ_* specify the position of an arbitrary point of the cylinder relative to O, C and the center of the image inclusion

4 Total stress and displacement fields

The total stresses are obtained as the sum of the infinite-medium and auxiliary stress fields, according to (1). Outside the inclusion, from (5) and (17), it follows that

$$\begin{aligned}
\sigma^{\text{out}}_{zr}(r,\theta) &= -\frac{\mu b^2}{\rho^4}\left\{\left[(d^2+r^2)\cos\theta - 2dr\right]\epsilon^{\bullet}_{zx} - \left[(d^2-r^2)\sin\theta\right]\epsilon^{\bullet}_{zy}\right\} \\
&\quad - \frac{\mu b_*^2}{\rho_*^4}\left\{\left[(d_*^2+r^2)\cos\theta - 2d_*r\right]\epsilon^{*}_{zx} - \left[(d_*^2-r^2)\sin\theta\right]\epsilon^{*}_{zy}\right\}, \\
\sigma^{\text{out}}_{z\theta}(r,\theta) &= \frac{\mu b^2}{\rho^4}\left\{\left[(d^2-r^2)\sin\theta\right]\epsilon^{\bullet}_{zx} + \left[(d^2+r^2)\cos\theta - 2dr\right]\epsilon^{\bullet}_{zy}\right\} \\
&\quad + \frac{\mu b_*^2}{\rho_*^4}\left\{\left[(d_*^2-r^2)\sin\theta\right]\epsilon^{*}_{zx} + \left[(d_*^2+r^2)\cos\theta - 2d_*r\right]\epsilon^{*}_{zy}\right\}.
\end{aligned} \tag{21}$$

In particular, the circumferential shear stress along the boundary of the void is

$$\sigma^{\text{out}}_{z\theta}(a,\theta) = \frac{2\mu b^2}{\rho_a^4}\left\{\left[(d^2-a^2)\sin\theta\right]\epsilon^{\bullet}_{zx} + \left[(d^2+a^2)\cos\theta - 2ad\right]\epsilon^{\bullet}_{zy}\right\} \tag{22}$$

where $\rho_a^2 = a^2 + d^2 - 2ad\cos\theta$, which is twice the circumferential shear stress along the corresponding circle in an infinite medium without the void, in accord with the general result of the antiplane strain elasticity established in [32]. The corresponding result for the plane strain elasticity was previously derived in [44].

Figure 4 shows the variation of the shear stress $\sigma^{\text{out}}_{z\theta}(a,\theta)$ around the void in the case when the inclusion (of the same radius as the void) is away from the void ($d = 3a$) and when it is touching the void ($d = 2a$). In both cases, the inclusion is characterized by equal eigenstrain components $\epsilon^{\bullet}_{zx} = \epsilon^{\bullet}_{zy}$. The pronounced stress amplification occurs as the inclusion approaches the void.

Inside the inclusion, from (9) and (17), the stresses are

$$\begin{aligned}
\sigma^{\text{in}}_{zr}(r,\theta) &= -\mu(\epsilon^{\bullet}_{zx}\cos\theta + \epsilon^{\bullet}_{zy}\sin\theta) \\
&\quad - \frac{\mu b_*^2}{\rho_*^4}\left\{\left[(d_*^2+r^2)\cos\theta - 2d_*r\right]\epsilon^{*}_{zx} - \left[(d_*^2-r^2)\sin\theta\right]\epsilon^{*}_{zy}\right\}, \\
\sigma^{\text{in}}_{z\theta}(r,\theta) &= -\mu(\epsilon^{\bullet}_{zy}\cos\theta - \epsilon^{\bullet}_{zx}\sin\theta) \\
&\quad + \frac{\mu b_*^2}{\rho_*^4}\left\{\left[(d_*^2-r^2)\sin\theta\right]\epsilon^{*}_{zx} + \left[(d_*^2+r^2)\cos\theta - 2d_*r\right]\epsilon^{*}_{zy}\right\}.
\end{aligned} \tag{23}$$

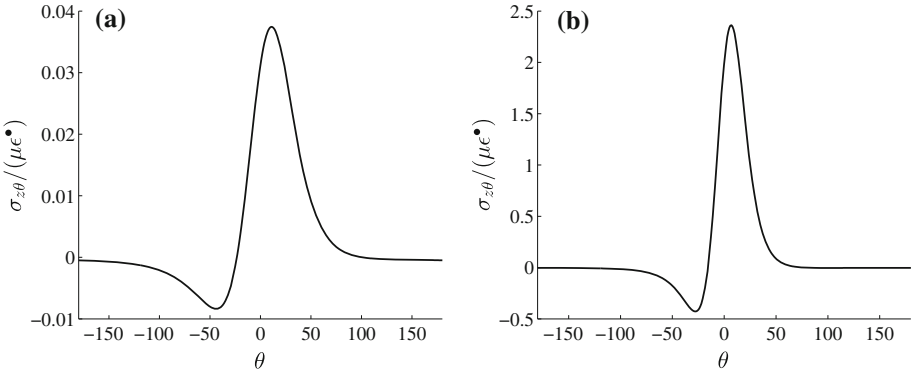

Fig. 4 The variation of stress $\sigma_{z\theta}(a,\theta)$ along the free surface of the void of radius a due to an inclusion of radius $b = a$ with its center at: **a** $d = 3a$, and **b** $d = 2a$ (inclusion tangent to the void). The *plots* correspond to $\epsilon^\bullet_{zx} = \epsilon^\bullet_{zy} = \epsilon^\bullet$

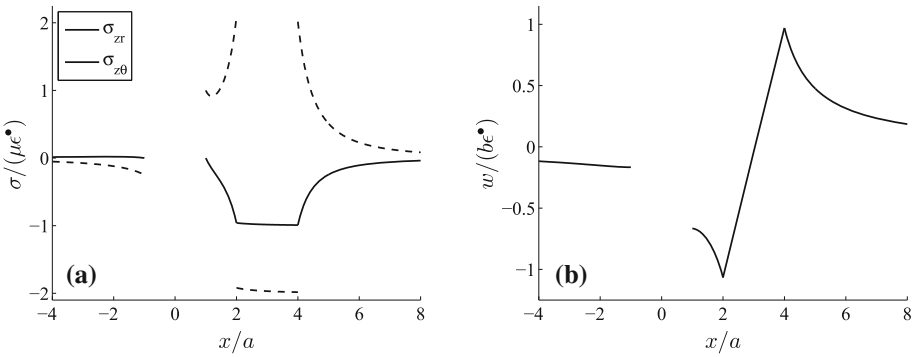

Fig. 5 **a** The variation of the stress components along the x-axis in the cases $d = 3a$. The radii of the void and inclusion are equal to each other ($b = a$), $\epsilon^\bullet_{zy} = 2\epsilon^\bullet$, and $\epsilon^\bullet_{zx} = \epsilon^\bullet$. **b** The variation of the corresponding displacement

The corresponding displacements are obtained by substituting (7), (10), and (20) into (2). The result is

$$w^{\text{out}}(r,\theta) = \frac{b^2}{\rho^2}\left[(r\cos\theta - d)\epsilon^\bullet_{zx} + (r\sin\theta)\epsilon^\bullet_{zy}\right] + \frac{b_*^2}{\rho_*^2}\left[(r\cos\theta - d_*)\epsilon^*_{zx} + (r\sin\theta)\epsilon^*_{zy}\right] + C_2,$$
$$w^{\text{in}}(r,\theta) = (r\cos\theta - d)\epsilon^\bullet_{zx} + (r\sin\theta)\epsilon^\bullet_{zy} + \frac{b_*^2}{\rho_*^2}\left[(r\cos\theta - d_*)\epsilon^*_{zx} + (r\sin\theta)\epsilon^*_{zy}\right] + C_2. \tag{24}$$

The angle θ for the field inside the inclusion is in the range $|\theta| \le \arcsin(b/d)$. If the condition is imposed that the displacement vanishes at infinity, the constant $C_2 = 0$. Figures 5a and 6a show the variation of the stress components $\sigma_{zr} = \sigma_{zx}$ and $\sigma_{z\theta} = \sigma_{zy}$ along the x-axis in the cases $d = 3a$ and $d = 2a$, if the radii of the void and inclusion are equal to each other ($b = a$) and $\epsilon^\bullet_{zy} = 2\epsilon^\bullet_{zx}$. In the latter case ($d = 2a$), the inclusion touches the void at $x = a$. The shear stresses σ_{zx} and σ_{zy} both relax to zero at the contact point and vary within the inclusion in a strongly nonlinear manner, in contrast to their almost linear variation with x in the case $d = 3a$. A similar observation is made for the displacement variation within the inclusion, shown in Figs. 5b and 6b. The stress discontinuity of σ_{zy} at $x = d \pm b$ is of magnitude $2\mu\epsilon^\bullet_{zy}$.

4.1 Inclusion in a circular cylinder

The preceding analysis also delivers the solution for an inclusion within a circular cylinder, whose boundary $r = a$ is traction-free (Fig. 7). The stresses and displacements inside and outside the inclusion are again given by expressions (21)–(24), with the geometric parameters as indicated in Fig. 7. The circumferential shear stress along the boundary of the cylinder is $\sigma_{z\theta}(a,\theta) = 2\sigma^0_{z\theta}(a,\theta)$, where $\sigma^0_{z\theta}(a,\theta)$ is the circumferential shear stress along $r = a$ corresponding to the inclusion in an infinite medium. The plots of the shear stress $\sigma_{z\theta}(a,\theta)$, for the configurations from Fig. 8, are shown in Fig. 9. The stress amplification increases as the inclusion moves

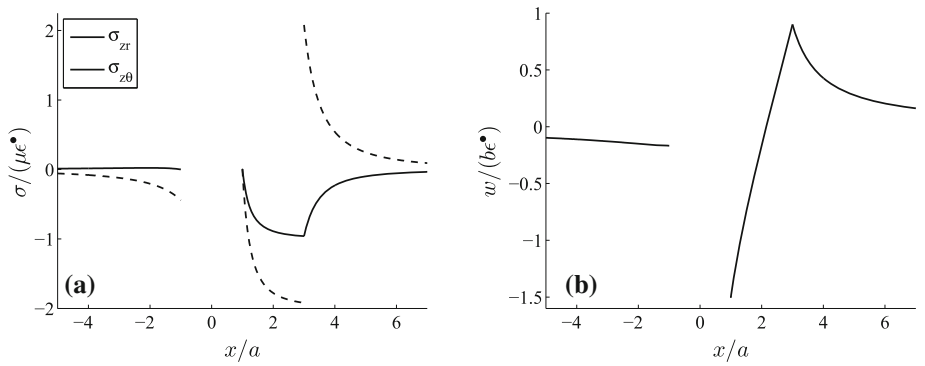

Fig. 6 **a** The variation of the stress components along the x-axis in the cases $d = 2a$, so that the inclusion touches the void. The radii of the void and inclusion are equal to each other ($b = a$), $\epsilon^{\bullet}_{zy} = 2\epsilon^{\bullet}$, and $\epsilon^{\bullet}_{zx} = \epsilon^{\bullet}$. **b** The variation of the corresponding displacement

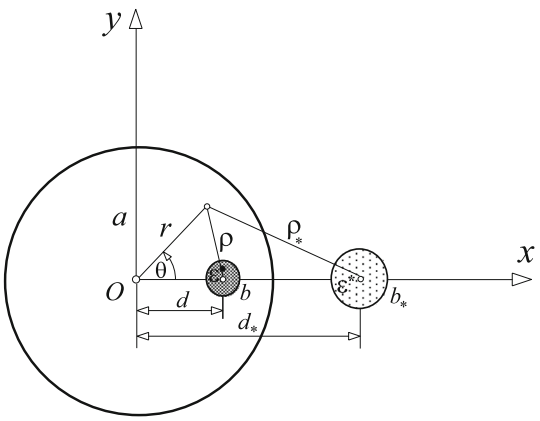

Fig. 7 Circular cylinder of radius a with the inserted inclusion of radius b and eigenstrains $(\epsilon^{\bullet}_{zx}, \epsilon^{\bullet}_{zy})$. The center of image inclusion of radius $b_* = (a/d)b$ and eigenstrains $(-\epsilon^{\bullet}_{zx}, \epsilon^{\bullet}_{zy})$ is at distance $d_* = a^2/d$ from the center of the cylinder, where d specifies the center of the actual inclusion. The radii r, ρ and ρ_* specify the position of an arbitrary point of the cylinder relative to O, C and the center of image inclusion

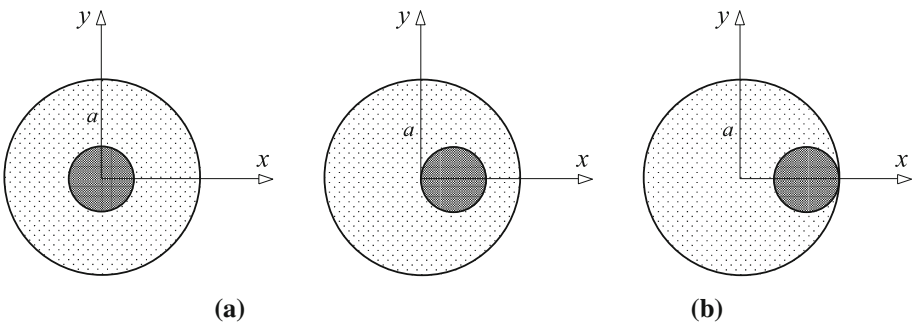

Fig. 8 Circular cylinder of radius a with the inserted inclusion of radius $b = a/3$ and eigenstrains $\epsilon^{\bullet}_{zx} = \epsilon^{\bullet}_{zy} = \epsilon^{\bullet}$. The center of the inclusion is at the distance: **a** $d = 0$, **b** $d = a/3$, and $d = 2a/3$ from the center of the cylinder

away from the center of the cylinder. Figure 9b shows the most pronounced stress amplification in the case when the inclusion is tangent to the cylinder. The stress amplification is localized in the region around $\theta = 0$. The circumferential shear stress at $\theta = 0$ is

$$\sigma^{\text{out}}_{z\theta}(a, 0) = 2\mu\epsilon^{\bullet}_{z\theta}\,\frac{b^2}{(a-d)^2}. \tag{25}$$

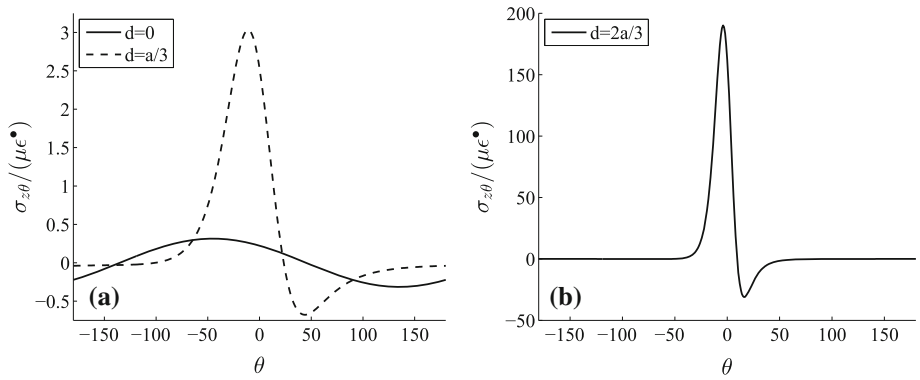

Fig. 9 The variation of stress $\sigma_{z\theta}(a,\theta)$ along the free surface of the cylinder with the inserted inclusion of radius $b=a$ with its center at: **a** $d=0$ and $d=a/3$, and **b** $d=2a/3$, as shown in Fig. 8. The *plots* correspond to $\epsilon^\bullet_{zx}=\epsilon^\bullet_{zy}=\epsilon^\bullet$

In the case $d=0$ (inclusion concentric with the cylinder), the stress expressions (21) and (23) simplify to

$$\sigma^{\text{out}}_{zr}(r,\theta)=\mu\epsilon^\bullet_{zr}\left(\frac{b^2}{a^2}-\frac{b^2}{r^2}\right),\quad \sigma^{\text{out}}_{z\theta}(r,\theta)=\mu\epsilon^\bullet_{z\theta}\left(\frac{b^2}{a^2}+\frac{b^2}{r^2}\right), \tag{26}$$

$$\sigma^{\text{in}}_{zr}(r,\theta)=\mu\epsilon^\bullet_{zr}\left(\frac{b^2}{a^2}-1\right),\quad \sigma^{\text{in}}_{z\theta}(r,\theta)=\mu\epsilon^\bullet_{z\theta}\left(\frac{b^2}{a^2}-1\right) \tag{27}$$

where $\epsilon^\bullet_{zr}=\epsilon^\bullet_{zx}\cos\theta+\epsilon^\bullet_{zy}\sin\theta$ and $\epsilon^\bullet_{z\theta}=\epsilon^\bullet_{zy}\cos\theta-\epsilon^\bullet_{zx}\sin\theta$. The displacement expressions (24) simplify to

$$\begin{aligned} w^{\text{out}}(r,\theta)&=\frac{b^2}{r}\,\epsilon^\bullet_{zx}\cos\theta+\left(\frac{b^2}{a^2}+\frac{b^2}{r^2}\right)r\epsilon^\bullet_{zy}\sin\theta,\\ w^{\text{in}}(r,\theta)&=r\epsilon^\bullet_{zx}\cos\theta+\left(\frac{b^2}{a^2}+1\right)r\epsilon^\bullet_{zy}\sin\theta. \end{aligned} \tag{28}$$

The displacement is imposed to be zero at the center of the inclusion ($r=0$). If $\delta=a-b\ll b$, the dominant stress is $\sigma^{\text{out}}_{z\theta}\approx 2\mu\epsilon^\bullet_{z\theta}$. The stresses inside the inclusion are $\sigma^{\text{in}}_{zr}\approx -2(\delta/a)\mu\epsilon^\bullet_{zr}$ and $\sigma^{\text{in}}_{z\theta}\approx -2(\delta/a)\mu\epsilon^\bullet_{z\theta}$.

5 Complex potentials

The complex potential for the infinite-medium displacement field inside the inclusion, considered in Sect. 2.1, is $\Phi^{0,\text{in}}(z)=\mu(z-d)\varepsilon^\bullet$, where $z=x+iy$ and $\varepsilon^\bullet=\epsilon^\bullet_{zy}+i\epsilon^\bullet_{zx}$ is the complex state of eigenstrain. The potential $\Phi^{0,\text{in}}(z)$ is defined so that, relative to the initial state before the stress-free eigenstrain transformation took place, the displacement $w^{0,\text{in}}=(1/\mu)\Im[\Phi^{0,\text{in}}(z)]$, where $\Im$ denoted the imaginary part. The stresses follow from $\sigma^{0,\text{in}}_{zy}+i\sigma^{0,\text{in}}_{zx}=\mathrm{d}[\Phi^{0,\text{in}}(z)-\Phi^\bullet(z)]/\mathrm{d}z$, with $\Phi^\bullet(z)=2\mu(z-d)\varepsilon^\bullet$ as the potential for the eigenstrain displacement $w^\bullet(z)=(1/\mu)\Im[\Phi^\bullet(z)]$. The complex potential for the infinite-medium field outside the inclusion is $\Phi^{0,\text{out}}(z)=-\mu b^2\overline{\varepsilon}^\bullet/(z-d)$, where the overline denotes the complex conjugate. The displacement is $w^{0,\text{out}}=(1/\mu)\Im[\Phi^{0,\text{out}}(z)]$, while the stress components follow from $\sigma^{0,\text{out}}_{zy}+i\sigma^{0,\text{out}}_{zx}=\mathrm{d}\Phi^{0,\text{out}}(z)/\mathrm{d}z$. Its polar components are deduced from $\sigma^{0,\text{out}}_{z\theta}+i\sigma^{0,\text{out}}_{zr}=(\sigma^{0,\text{out}}_{zy}+i\sigma^{0,\text{out}}_{zx})\exp(i\theta)$. In the above derivation, it may be noted that, by the circle theorem, $\Phi^{0,\text{out}}(\zeta)=-\overline{\Phi}^{\,0,\text{in}}(b^2/\zeta)$, where $\zeta=z-d$.

The complex potential for the auxiliary field can be determined from $\hat{\Phi}(z)=-\overline{\Phi}^{\,0,\text{out}}(a^2/z)$, which gives

$$\hat{\Phi}(z)=\mu b^2\,\frac{z\varepsilon^\bullet}{a^2-dz}=-\mu b_*^2\,\frac{\overline{\varepsilon}^*}{z-d_*}-\mu\frac{b^2}{d}\,\overline{\varepsilon}^\bullet,\quad \overline{\varepsilon}^*=\varepsilon^\bullet. \tag{29}$$

The complex potential for the overall field outside the inclusion is $\Phi^{\text{out}}(z)=\Phi^{0,\text{out}}(z)+\hat{\Phi}(z)$, i.e.,

$$\Phi^{\text{out}}(z)=\mu b^2\left(-\frac{\overline{\varepsilon}^\bullet}{z-d}+\frac{z\varepsilon^\bullet}{a^2-dz}\right)=-\mu b^2\,\frac{\overline{\varepsilon}^\bullet}{z-d}-\mu b_*^2\,\frac{\overline{\varepsilon}^*}{z-d_*}-\mu\frac{b^2}{d}\,\overline{\varepsilon}^\bullet. \tag{30}$$

The stress components follow from $\sigma_{zy}^{\text{out}} + i\sigma_{zx}^{\text{out}} = \mathrm{d}\Phi^{\text{out}}(z)/\mathrm{d}z$, while the displacement is $w^{\text{out}} = (1/\mu)\Im[\Phi^{\text{out}}(z)]$, up to an arbitrary constant.

The complex potential for the overall field inside the inclusion is $\Phi^{\text{in}}(z) = \Phi^{0,\text{in}}(z) + \hat{\Phi}(z)$. This gives

$$\Phi^{\text{in}}(z) = \mu(z-d)\varepsilon^{\bullet} + \mu b^2 \frac{z\varepsilon^{\bullet}}{a^2 - dz} = \mu(z-d)\varepsilon^{\bullet} - \mu b_*^2 \frac{\overline{\varepsilon}^*}{z - d_*} - \mu \frac{b^2}{d}\overline{\varepsilon}^{\bullet}. \tag{31}$$

The displacement is $w^{\text{in}} = (1/\mu)\Im[\Phi^{\text{in}}(z)]$, up to the same constant as in the expression for w^{out}, in order to preserve the continuity of displacement across the boundary of the inclusion. The stresses within the inclusion follow from $\sigma_{zy}^{\text{in}} + i\sigma_{zx}^{\text{in}} = \mathrm{d}[\Phi^{\text{in}}(z) - \Phi^{\bullet}(z)]/\mathrm{d}z$.

5.1 Remarks on the extended circle theorem

The Milne–Thomson circle theorem for irrotational two-dimensional flow of incompressible inviscid fluid [29,30] has been first applied to solid mechanics problems by Smith [31] in his study of the interaction between screw dislocations and circular inhomogeneities, and by Lin et al. [32] in their study of elastic materials with damage zones. In particular, the latter authors list the following formulas for the stress components in the matrix, outside the circular inhomogeneity in an infinite medium, due to the source of stress, which is outside the inhomogeneity:

$$\sigma_{zr}^{\text{M}}(r,\theta) = \sigma_{zr}^{0}(r,\theta) + \lambda \frac{a^2}{r^2}\sigma_{zr}^{0}\left(a^2/r,\theta\right), \quad \sigma_{z\theta}^{\text{M}}(r,\theta) = \sigma_{z\theta}^{0}(r,\theta) - \lambda \frac{a^2}{r^2}\sigma_{z\theta}^{0}\left(a^2/r,\theta\right). \tag{32}$$

The superposed ^{0} designates the stress field in a homogeneous infinite medium, $\lambda = (\mu_{\text{I}} - \mu_{\text{M}})/(\mu_{\text{I}} + \mu_{\text{M}})$, and $(\mu_{\text{I}}, \mu_{\text{M}})$ are the shear moduli of the inhomogeneity and the matrix, respectively. The stress components (32) follow from the circle theorem: The complex potentials for the stress field inside and outside the inhomogeneity are $\Phi^{\text{I}}(z) = (1+\lambda)\Phi^{0}(z)$ and $\Phi^{\text{M}}(z) = \Phi^{0}(z) + \lambda\overline{\Phi}^{0}(a^2/z)$, where $\Phi^{0}(z)$ is the complex potential of the homogeneous problem. Referring to relations (32), it is stated in [32] that "the relations are universal in the sense of being independent of any particular loading." While this statement is fully applicable to many problems, such as those of screw dislocation or concentrated line force near an inhomogeneity, or an inhomogeneity in an infinite medium under remote loading, it does not apply to the problem of an eigenstrain inclusion near an inhomogeneity, because the relations (32) deliver correctly only the stresses outside but not inside the inclusion. Indeed, if the inhomogeneity is a void ($\lambda = -1$), they yield within the inclusion the incorrect field

$$\sigma_{zr}^{\text{in}}(r,\theta) = -\mu\epsilon_{zr}^{\bullet}\left(1 - \frac{a^2}{r^2}\right), \quad \sigma_{z\theta}^{\text{in}}(r,\theta) = -\mu\epsilon_{z\theta}^{\bullet}\left(1 + \frac{a^2}{r^2}\right), \tag{33}$$

rather than the correct field specified by the expressions (23) from Sect. 4.

The remark made in this section is cautionary, relevant for the case when the cause of stress is an eigenstrain inclusion. The wide applicability of the extended circle theorem to other antiplane strain elasticity problems is remarkable, as demonstrated by Honein et al. [13,14] in their comprehensive analysis of two or more inhomogeneities under remote or other type of loadings by the procedure they refer to as the heterogenization.

6 Inclusion in a half-space

If the inclusion is near the free surface of a half-space (Fig. 10a), the image inclusion is positioned symmetrically with respect to the boundary of a half-space, its radius is equal to the radius of actual inclusion (b), and its eigenstrain is $(\epsilon_{zx}^{*}, \epsilon_{zy}^{*}) = (-\epsilon_{zx}^{\bullet}, \epsilon_{zy}^{\bullet})$. This can be compared with the well-known cases of screw dislocation near the free surface of a half-space, where the opposite image screw dislocation is placed at the mirror position across the free surface, and a concentrated line force near the free surface of a half-space, where the image line force of the same sign is placed at the mirror position across the free surface [33–35]. The displacements inside and outside the inclusion are

$$w^{\text{in}} = \left[(x-c)\epsilon_{zx}^{\bullet} + y\epsilon_{zy}^{\bullet}\right] + \frac{b^2}{\rho_*^2}\left[(x+c)\epsilon_{zx}^{*} + y\epsilon_{zy}^{*}\right], \tag{34}$$

$$w^{\text{out}} = \frac{b^2}{\rho^2}\left[(x-c)\epsilon_{zx}^{\bullet} + y\epsilon_{zy}^{\bullet}\right] + \frac{b^2}{\rho_*^2}\left[(x+c)\epsilon_{zx}^{*} + y\epsilon_{zy}^{*}\right] \tag{35}$$

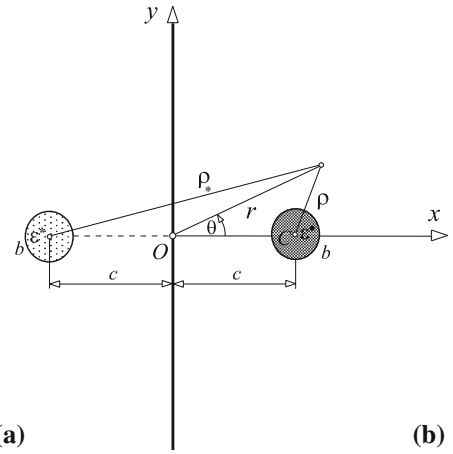

Fig. 10 A circular inclusion of radius b with its center at distance c from the free surface $x = 0$ of a half-space. The image inclusion of the same radius is at the mirror image location, characterized by the eigenstrain $(\epsilon^*_{zx}, \epsilon^*_{zy}) = (-\epsilon^\bullet_{zx}, \epsilon^\bullet_{zy})$

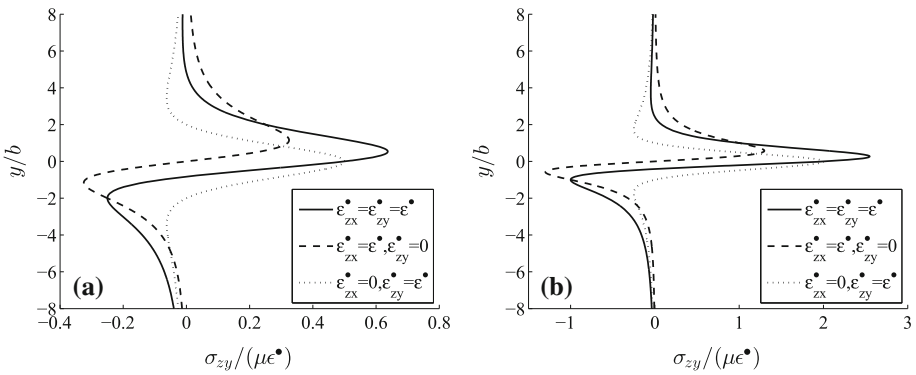

Fig. 11 The variation of stress $\sigma_{zy}(0, y)$ along the free surface of a half-space due to inclusion of radius b with its center at: **a** $c = 2b$, and **b** $c = b$. The *plots* correspond to three selected ratios of $\epsilon^\bullet_{zx}$ and $\epsilon^\bullet_{zy}$

where $\rho^2 = (x - c)^2 + y^2$ and $\rho_*^2 = (x + c)^2 + y^2$. The corresponding complex potentials are

$$\Phi^{\text{in}}(z) = \mu\varepsilon^\bullet\left(z - c - \frac{b^2}{z + c}\right), \quad \Phi^{\text{out}}(z) = -\frac{\mu b^2}{z - c}\,\bar{\varepsilon}^\bullet - \frac{\mu b^2}{z + c}\,\varepsilon^\bullet. \tag{36}$$

The complex potential for the eigenstrain displacement is $\Phi^\bullet(z) = 2\mu(z - c)\varepsilon^\bullet$, such that $\sigma^{\text{in}}_{zy} + i\sigma^{\text{in}}_{zx} = \mathrm{d}[\Phi^{\text{in}}(z) - \Phi^\bullet(z)]/\mathrm{d}z$, while $w^{\text{in}} = (1/\mu)\Im[\Phi^{\text{in}}(z)]$.

In particular, the nonvanishing shear stress along the free surface is

$$\sigma_{zy}(0, y) = 2\sigma^0_{zy}(0, y) = \frac{2\mu b^2}{(c^2 + y^2)^2}\left[2cy\epsilon^\bullet_{zx} + (c^2 - y^2)\epsilon^\bullet_{zy}\right]. \tag{37}$$

This is plotted in Fig. 11 in the cases $c = 2b$ and $c = b$, for various ratios of $\epsilon^\bullet_{zx}$ and $\epsilon^\bullet_{zy}$. In the case $c = b$, the inclusion touches the free surface at $x = 0$. In this case, there is a significant buildup of stress near $y = 0$, albeit the stress diminishes with y more rapidly than for $c > b$. Also, for $\epsilon^\bullet_{zx} = 0$ and $\epsilon^\bullet_{zy} > 0$, there is a buildup of negative σ_{zy} within $|y| < c$, reaching the maximum magnitude $\mu(b/2c)^2$ at $y = \pm\sqrt{3}c$. In general, the curves are symmetric with respect to $y = 0$ in the case $\epsilon^\bullet_{zx} = 0$, antisymmetric in the case $\epsilon^\bullet_{zy} = 0$, and asymmetric in the case when both $\epsilon^\bullet_{zx}$ and $\epsilon^\bullet_{zy}$ are nonzero.

The variation of the corresponding surface displacement, determined from

$$w(0, y) = \frac{2b^2}{c^2 + y^2}\,(y\epsilon^\bullet_{zy} - c\epsilon^\bullet_{zx}), \tag{38}$$

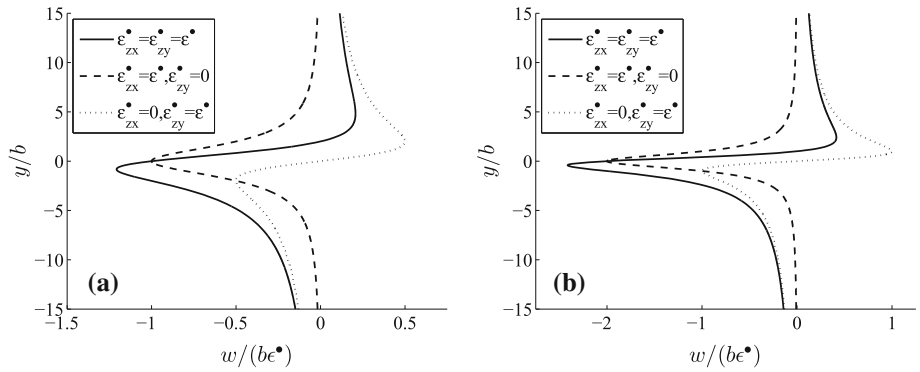

Fig. 12 The variation of the displacement $w(0, y)$ along the free surface of a half-space due to an inclusion of radius b with its center at: **a** $c = 2b$, and **b** $c = b$. The *plots* correspond to three selected ratios of $\epsilon^{\bullet}_{zx}$ and $\epsilon^{\bullet}_{zy}$

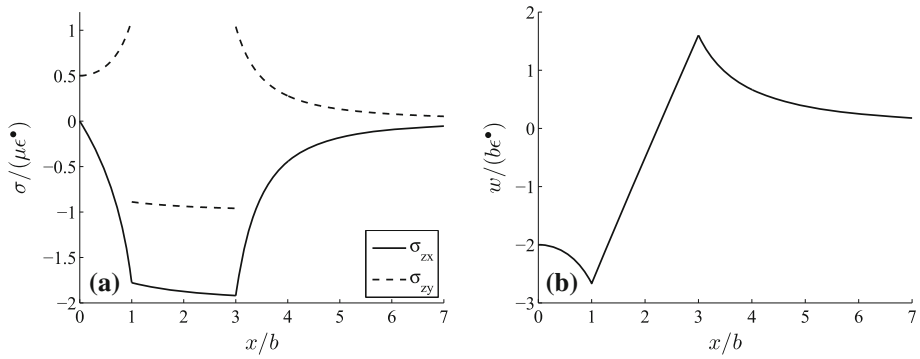

Fig. 13 **a** The variation of stress components along the x-axis in the cases $c = 2b$, $\epsilon^{\bullet}_{zx} = 2\epsilon^{\bullet}$, and $\epsilon^{\bullet}_{zy} = \epsilon^{\bullet}$. **b** The corresponding displacement variation

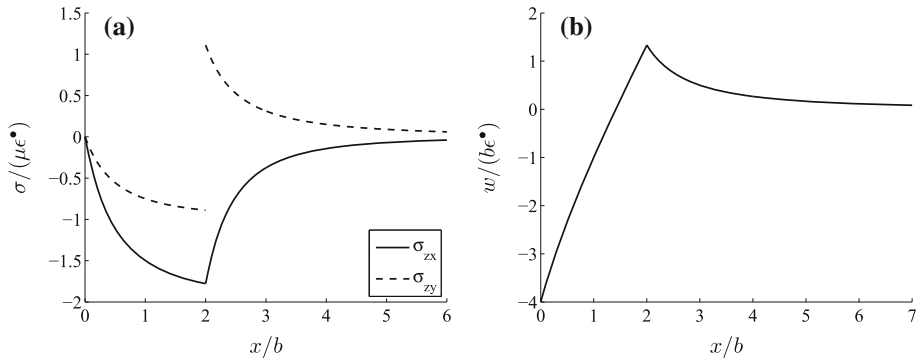

Fig. 14 **a** The variation of stress components along the x-axis in the cases $c = b$, $\epsilon^{\bullet}_{zx} = 2\epsilon^{\bullet}$, and $\epsilon^{\bullet}_{zy} = \epsilon^{\bullet}$. **b** The corresponding displacement variation

is shown in Fig. 12. Both the stress components and the displacement are proportional to $(b/c)^2$, so that doubling the radius of the inclusion at fixed c quadruples their values.

Figures 13a and 14a show the variation of the stress components and the displacement along the x-axis in the cases $c = 2b$ and $c = b$, if $\epsilon^{\bullet}_{zx} = 2\epsilon^{\bullet}_{zy}$. The stress discontinuity of σ_{zy} at $x = c \pm b$ is of magnitude $2\mu\epsilon^{\bullet}_{zy}$, as in the infinite medium. The corresponding displacement variations are shown in Figs. 13b and 14b. The displacement vanishes as $x \to \pm\infty$, while at $x = 0$ the displacement is $-(2b^2/c)\epsilon^{\bullet}_{zx}$.

7 Configurational forces between a circular inclusion and a void

We next evaluate the configurational forces on the void and inclusion due to changes in their relative position or their radii, caused by diffusional or diffusionless processes and transformations within the material, without explicitly accounting for the origin and details of such physical changes. The J_x integral for the antiplane strain infinitesimal deformations is defined in terms of the Eshelby stress tensor $P_{\alpha x}$ by [45]

$$J_x = \oint (P_{xx} n_x + P_{yx} n_y)\, \mathrm{d}l, \quad P_{\alpha x} = W\delta_{\alpha x} - \sigma_{z\alpha} u_{z,x}, \quad (\alpha = x, y), \tag{39}$$

where $\delta_{\alpha\beta}$ denotes the Kronecker delta, and $\mathrm{d}l$ is an infinitesimal arc length. For linear elasticity, the strain energy density is $W = (\sigma_{zx}^2 + \sigma_{zy}^2)/(2\mu)$. Expressed in cylindrical coordinates, (39) can be cast in the form

$$J_x = \frac{r}{2\mu} \oint \left[(\sigma_{z\theta}^2 - \sigma_{zr}^2) \cos\theta + 2\sigma_{zr}\sigma_{z\theta} \right] \mathrm{d}\theta. \tag{40}$$

When evaluated over a closed contour which does not embrace a singularity or a defect, the integral in (40) vanishes. Such contour is a closed contour around the void and inclusion, along the positive x axis, and around a remote circle of large radius $R \gg (a, b, d)$, as shown in Fig. 15. The contributions to J_x along the lines just above and below the x-axis cancel each other, and the contribution from the remote circle vanishes because stresses fall off as $1/R^2$ in the limit $R \to \infty$, as in an unvoided infinite medium (at large R, the stress field is increasingly unaware of the presence of a void near the inclusion). Thus, $J_x = J_x^{\text{void}} + J_x^{\text{incl}} = 0$, i.e.,

$$J_x^{\text{incl}} = -J_x^{\text{void}}. \tag{41}$$

The J_x integral along the boundary of the void is

$$J_x^{\text{void}} = \frac{a}{2\mu} \int_0^{2\pi} \sigma_{z\theta}^2(a, \theta) \cos\theta \, \mathrm{d}\theta, \tag{42}$$

because $\sigma_{zr}(a, \theta) = 0$ in (40) along the circumference of the void. By incorporating the stress expression (6) into (42), there follows

$$\begin{aligned} J_x^{\text{void}} = 4\mu a b^4 \Big\{ & \left[(d^2 - a^2)^2 I_1 \right] \epsilon_{zx}^{\bullet 2} \\ & + \left[4d^2 a^2 I_2 - 4da(d^2 + a^2) I_3 + (d^2 + a^2)^2 I_4 \right] \epsilon_{zy}^{\bullet 2} \Big\}. \end{aligned} \tag{43}$$

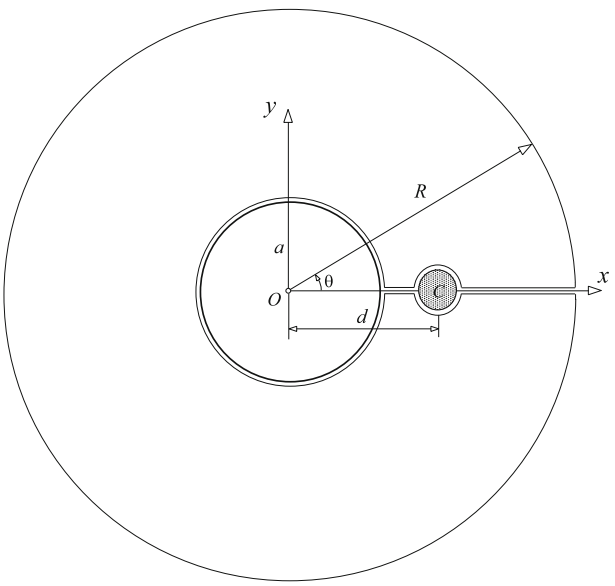

Fig. 15 The closed contour around the void of radius a with its center at O, and the inclusion of radius b with its center at C, used to evaluate the J and M integrals. The radius of the remote circle $R \to \infty$

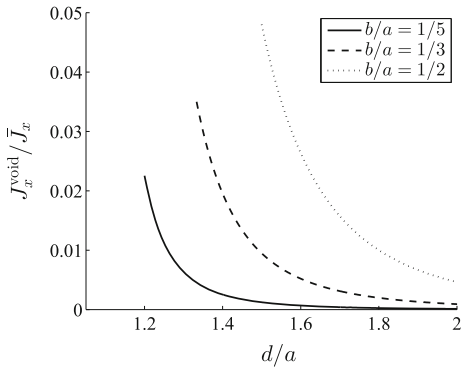

Fig. 16 The variation of the configurational force J_x^{void} with d/a for indicated values of the ratio b/a. The scaling force parameter is $\bar{J}_x = 4\pi\mu a(\epsilon_{zx}^{\bullet 2} + \epsilon_{zy}^{\bullet 2})$. At far distances from the void, the configurational force J_x^{void} tends to zero as $(d/a)^{-1}$. The left endpoints of the curves $(d/a = 1 + b/a)$ specify the maximum configurational force corresponding to a selected value of ratio b/a, which is given by (45)

The integrals appearing in (43) are specified and evaluated in "Appendix B" of the paper. The coefficients in front of $\epsilon_{zx}^{\bullet 2}$ and $\epsilon_{zy}^{\bullet 2}$ are equal to each other, so that (43) becomes

$$J_x^{\text{void}} = 4\pi\mu(b/a)^4 \frac{d}{[(d/a)^2 - 1]^3}\left(\epsilon_{zx}^{\bullet 2} + \epsilon_{zy}^{\bullet 2}\right), \quad d \geq (a+b). \tag{44}$$

This represents the energy release rate associated with an imagined void translation within the material toward the inclusion (by diffusion or otherwise), keeping the position of the inclusion fixed, i.e., the material or configurational force on the void exerted by the inclusion. An interesting outcome of the analysis is that the configurational force between the void and inclusion depends only on the magnitude of total eigenstrain, and not on the ratio of the eigenstrain components. Thus, the force is the same if a given amount of eigenstrain is applied as either $\epsilon_{zx}^{\bullet}$ or $\epsilon_{zy}^{\bullet}$. The force on the inclusion exerted by the void is equal in magnitude and opposite in direction. The maximum value of the force on the void is reached at the minimum distance ($d_{\min} = a + b$) between the centers of the inclusion and void for which the presented analysis applies. This force is

$$J_{x,\max}^{\text{void}} = 4\pi\mu b \frac{1 + b/a}{(2 + b/a)^3}\left(\epsilon_{zx}^{\bullet 2} + \epsilon_{zy}^{\bullet 2}\right). \tag{45}$$

The variation of J_x^{void} with d/a for several values of b/a is shown in Fig. 16.

7.1 Total strain energy

The total strain energy in the medium with the inserted inclusion near a traction-free void is the sum of the strain energy term corresponding to an inclusion inserted in an infinite medium far away from the void, which is given by (4), and the term dependent on d, which accounts for the interaction between the void and inclusion,

$$E_T = \pi\mu b^2\left(\epsilon_{zx}^{\bullet 2} + \epsilon_{zy}^{\bullet 2}\right) + \hat{E}_T(d, b). \tag{46}$$

The energy $\hat{E}_T$ can be conveniently determined by noting that its negative gradient with respect to the distance between the inclusion and the (fixed) void must be equal to the configurational force on the inclusion, i.e., in view of (41) and (44),

$$\frac{\partial \hat{E}_T}{\partial d} = 4\pi\mu\left(\epsilon_{zx}^{\bullet 2} + \epsilon_{zy}^{\bullet 2}\right)\frac{adb^4}{(d^2 - a^2)^3}. \tag{47}$$

Upon integration, this gives

$$\hat{E}_T = -\pi\mu\left(\epsilon_{zx}^{\bullet 2} + \epsilon_{zy}^{\bullet 2}\right)\frac{a^2b^4}{(d^2 - a^2)^2}, \tag{48}$$

up to an immaterial constant term. Consequently, by substituting (48) into (46), the total strain energy becomes

$$E_T = \pi\mu b^2\left(\epsilon_{zx}^{\bullet 2}+\epsilon_{zy}^{\bullet 2}\right)\left[1-\frac{a^2b^2}{(d^2-a^2)^2}\right]. \tag{49}$$

The following quantities are also evaluated from (49):

$$-a\frac{\partial E_T}{\partial a} = 2\pi\mu a^2\left(\epsilon_{zx}^{\bullet 2}+\epsilon_{zy}^{\bullet 2}\right)\left(\frac{b}{a}\right)^4\frac{(d/a)^2+1}{[(d/a)^2-1]^3}, \tag{50}$$

$$-b\frac{\partial E_T}{\partial b} = 2\pi\mu a^2\left(\epsilon_{zx}^{\bullet 2}+\epsilon_{zy}^{\bullet 2}\right)\left[-\left(\frac{b}{a}\right)^2+\left(\frac{b}{a}\right)^4\frac{2}{[(d/a)^2-1]^2}\right], \tag{51}$$

which will be compared with the M integrals evaluated in the next section.

8 M integral evaluation

From the general expressions given in [46,47], the M_O integral of antiplane shear, with respect to the coordinate origin at O, can be expressed as

$$M_O = \oint\left(P_{\alpha x}n_\alpha x + P_{\alpha y}n_\alpha y\right)\mathrm{d}l, \quad P_{\alpha\beta} = W\delta_{\alpha\beta} - \sigma_{z\alpha}u_{z,\beta}, \quad (\alpha,\beta = x,y), \tag{52}$$

with the sum on repeated α. Expressed in cylindrical coordinates, (52) becomes

$$M_O = \frac{r^2}{2\mu}\oint\left(\sigma_{z\theta}^2-\sigma_{zr}^2\right)\mathrm{d}\theta. \tag{53}$$

By using the same closed contour from Fig. 15 as in the evaluation of the J_x integral, the contribution from the remote circle $M_O^R \to 0$ as $R\to\infty$, because stresses decay as $1/R^2$ far away from the inclusion. Thus, $M_O^{\text{void}} + M_O^{\text{incl}} = 0$, where

$$M_O^{\text{void}} = \frac{a^2}{2\mu}\int_0^{2\pi}\sigma_{z\theta}^2(a,\theta)\,\mathrm{d}\theta. \tag{54}$$

Upon using the circumferential shear stress expression (6), the integration in (54) gives

$$\begin{aligned} M_O^{\text{void}} = 4\mu a^2b^4\Big\{&\left[(d^2-a^2)^2I_5\right]\epsilon_{zx}^{\bullet 2} \\ &+\left[4d^2a^2I_6 - 4da(d^2+a^2)I_2 + (d^2+a^2)^2I_3\right]\epsilon_{zy}^{\bullet 2}\Big\}. \end{aligned} \tag{55}$$

The integrals appearing in (55) are defined and evaluated in "Appendix B". Their substitution into (55) yields

$$M_O^{\text{void}} = 2\pi\mu a^2(b/a)^4\frac{(d/a)^2+1}{[(d/a)^2-1]^3}\left(\epsilon_{zx}^{\bullet 2}+\epsilon_{zy}^{\bullet 2}\right). \tag{56}$$

Physically, the ratio M_O^{void}/a represents the energy release rate associated with isotropic void growth (by material absorbtion over the surface of the void), keeping the position of the inclusion fixed relative to the center of the void. Indeed, the comparison of (56) with (50) shows that $M_O^{\text{void}} = -a(\partial E_T/\partial a)$.

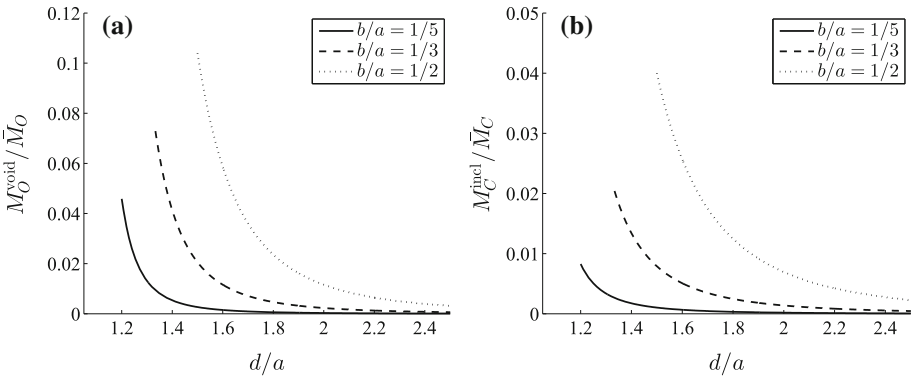

Fig. 17 The variation of **a** M_O^{void} and **b** M_C^{void} with d/a for indicated values of the ratio b/a. The scaling parameters for both plots are $\bar{M}_O = \bar{M}_C = 2\pi\mu a^2(\epsilon_{zx}^{\bullet 2} + \epsilon_{zy}^{\bullet 2})$. At far distances from the void, M_O^{void} and M_C^{void} approach zero as $(d/a)^{-4}$ and $(d/a)^{-2}$, respectively

8.1 **M** integral around inclusion

By using the well-known relationship between the M integrals relative to coordinate origins at O and C, one can write

$$M_O^{\text{incl}} = M_C^{\text{incl}} + d \cdot J_x^{\text{incl}}, \tag{57}$$

and from the relationship $M_O^{\text{void}} + M_O^{\text{incl}} = 0$, there follows

$$M_C^{\text{incl}} = -\left(M_O^{\text{void}} + d \cdot J_x^{\text{incl}}\right). \tag{58}$$

Thus, by substituting (56) and $J_x^{\text{incl}} = -J_x^{\text{void}}$ from (44), the M_C integral around the inclusion is found to be

$$M_C^{\text{incl}} = 2\pi\mu a^2 (b/a)^4 \frac{1}{[(d/a)^2 - 1]^2}\left(\epsilon_{zx}^{\bullet 2} + \epsilon_{zy}^{\bullet 2}\right). \tag{59}$$

If $d \gg a$, M_C^{incl} approaches zero, as if the inclusion was in an infinite medium without void. The variation of M_O^{void} and M_C^{void} with d/a for several values of ratio b/a is shown in Fig. 17. In the limiting case $d = a + b$, the two integrals are $M_{C,\max}^{\text{incl}} = 2\pi\mu(\epsilon_{zx}^{\bullet 2} + \epsilon_{zy}^{\bullet 2})b^2/(2 + b/a)^2$ and $M_{O,\max}^{\text{void}} = -M_{C,\max}^{\text{incl}} + (a + b) \cdot J_{x,\max}^{\text{void}}$.

8.2 Expansion of the inclusion

The M_C^{incl}/b is not proportional to the energy rate associated with isotropic growth (expansion) of the inclusion $(\partial E_T/\partial b)$, which is given in (51). If the specific configurational force (f) is introduced, the rate of total strain energy associated with uniform expansion of the inclusion can be expressed as [48]

$$\frac{\partial E_T}{\partial b} = -\int_0^{2\pi} f(b,\varphi) b \, \mathrm{d}\varphi, \quad f = \left[\frac{1}{2}\left(\sigma_{ij}^{0,\text{in}} + \sigma_{ij}^{0,\text{out}}\right)_{\rho=b} + \hat{\sigma}_{ij}(b,\varphi)\right]\epsilon_{ij}^{\bullet} \tag{60}$$

where $\hat{\sigma}_{ij}(b,\varphi)$ are the stress components of the auxiliary problem along the circumference of the inclusion $(\rho = b)$. The specific configurational force is thus

$$f = \left(\sigma_{zx}^{0,\text{in}} + \sigma_{zx}^{0,\text{out}}\right)_{\rho=b}\epsilon_{zx}^{\bullet} + \left(\sigma_{zy}^{0,\text{in}} + \sigma_{zy}^{0,\text{out}}\right)_{\rho=b}\epsilon_{zy}^{\bullet} + 2\left(\hat{\sigma}_{zx}\epsilon_{zx}^{\bullet} + \hat{\sigma}_{zy}\epsilon_{zy}^{\bullet}\right)_{\rho=b}. \tag{61}$$

From the infinite-medium stress expressions listed in Sect. 2.1, it follows that the first two terms in (61) are

$$\begin{aligned}&\left(\sigma_{zx}^{0,\text{in}} + \sigma_{zx}^{0,\text{out}}\right)_{\rho=b}\epsilon_{zx}^{\bullet} + \left(\sigma_{zy}^{0,\text{in}} + \sigma_{zy}^{0,\text{out}}\right)_{\rho=b}\epsilon_{zy}^{\bullet} \\ &\quad = -\mu\left[\epsilon_{zx}^{\bullet 2} + \epsilon_{zy}^{\bullet 2} + \left(\epsilon_{zx}^{\bullet 2} - \epsilon_{zy}^{\bullet 2}\right)\cos 2\varphi + 2\epsilon_{zx}^{\bullet}\epsilon_{zy}^{\bullet}\sin 2\varphi\right].\end{aligned} \tag{62}$$

Incorporating the expressions for the auxiliary stresses from Sect. 2.2, the third term on the right-hand side of (61) is found to be

$$2\left(\hat{\sigma}_{zx}\epsilon^{\bullet}_{zx}+\hat{\sigma}_{zy}\epsilon^{\bullet}_{zy}\right)_{\rho=b}=2\mu b_*^2\left(\epsilon^{\bullet\,2}_{zx}+\epsilon^{\bullet\,2}_{zy}\right)\left(\frac{1}{\rho_b^2}-2b^2\,\frac{\sin^2\varphi}{\rho_b^4}\right) \tag{63}$$

where $\rho_b^2=(d-d_*)^2+2(d-d_*)b\cos\varphi+b^2$, $d_*=a^2/d$, and $b_*=ab/d$. Thus, the local specific configurational force, orthogonal at each point to the circumference of the inclusion, is

$$\begin{aligned} f=&-\mu\left[\epsilon^{\bullet\,2}_{zx}+\epsilon^{\bullet\,2}_{zy}+\left(\epsilon^{\bullet\,2}_{zx}-\epsilon^{\bullet\,2}_{zy}\right)\cos 2\varphi+2\epsilon^{\bullet}_{zx}\epsilon^{\bullet}_{zy}\sin 2\varphi\right]\\ &+2\mu b_*^2\left(\epsilon^{\bullet\,2}_{zx}+\epsilon^{\bullet\,2}_{zy}\right)\left(\frac{1}{\rho_b^2}-2b^2\,\frac{\sin^2\varphi}{\rho_b^4}\right). \end{aligned} \tag{64}$$

The substitution of (64) into (60) and integration give the expression for the rate of energy associated with a uniform expansion of the inclusion,

$$\frac{\partial E_T}{\partial b}=2\pi\mu b\left(\epsilon^{\bullet\,2}_{zx}+\epsilon^{\bullet\,2}_{zy}\right)-4\pi\mu b\left(\epsilon^{\bullet\,2}_{zx}+\epsilon^{\bullet\,2}_{zy}\right)\frac{a^2b^2}{(d^2-a^2)^2}, \tag{65}$$

in agreement with (51). The second part of the above expression is recognized to be $\delta\hat{E}_T/\delta b$, where $\hat{E}_T$ was defined by (48). The comparison of (65) with the M integral around the inclusion (59) shows that

$$-\frac{\partial E_T}{\partial b}=-2\pi\mu b\left(\epsilon^{\bullet\,2}_{zx}+\epsilon^{\bullet\,2}_{zy}\right)+2\,\frac{M_C^{\rm incl}}{b}. \tag{66}$$

Thus, the energy release rate for a self-similarly expanding inclusion is not equal to the M_C/b ratio around the inclusion; cf. [8] where this distinction was not made.

9 Configurational forces on the inclusion in a circular cylinder and in a half-space

The preceding analysis delivers the expression for the configurational force on the inclusion within a circular cylinder whose boundary $r=a$ is traction-free (Fig. 7). This follows from (44) by replacing b with ab/d, and d with a^2/d. The result is

$$J_x^{\rm incl}=4\pi\mu(b/a)^4\,\frac{d}{[1-(d/a)^2]^3}\left(\epsilon^{\bullet\,2}_{zx}+\epsilon^{\bullet\,2}_{zy}\right),\quad d\le(a-b). \tag{67}$$

The rate of strain energy associated with a uniform expansion of the inclusion is given by (65). In the case of a concentric inclusion within a cylinder, the total strain energy is obtained from (49) by taking $d=0$, which gives

$$E_T=\pi\mu b^2\left(1-\frac{b^2}{a^2}\right)\left(\epsilon^{\bullet\,2}_{zx}+\epsilon^{\bullet\,2}_{zy}\right). \tag{68}$$

This can also be independently derived by integration from

$$E_T=\frac{1}{2\mu}\left[\int_0^{2\pi}\int_0^b\left(\sigma^{0,\rm in\ 2}_{z\rho}+\sigma^{0,\rm in\ 2}_{z\varphi}\right)\rho\,{\rm d}\rho\,{\rm d}\varphi+\int_0^{2\pi}\int_b^a\left(\sigma^{0,\rm out\ 2}_{z\rho}+\sigma^{0,\rm out\ 2}_{z\varphi}\right)\rho\,{\rm d}\rho\,{\rm d}\varphi\right] \tag{69}$$

where the stresses are specified by (26) and (27). The M integral around the concentric inclusion is $M_C^{\rm incl}=2\pi\mu(b^2/a)^2\left(\epsilon^{\bullet\,2}_{zx}+\epsilon^{\bullet\,2}_{zy}\right)$, while the specific configurational force and the energy release rate are

$$f=-\mu\left(1-2\,\frac{b^2}{a^2}\right)\left(\epsilon^{\bullet\,2}_{zx}+\epsilon^{\bullet\,2}_{zy}\right),\quad -\frac{\partial E_{\rm T}}{\partial b}=2\pi bf,\quad b\le a. \tag{70}$$

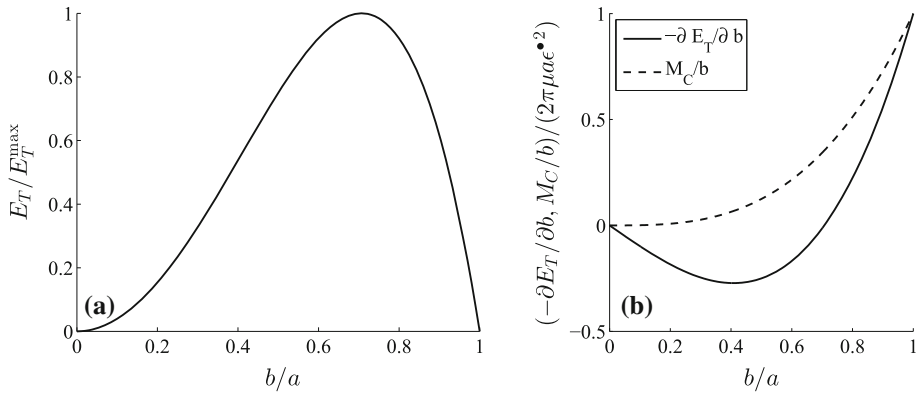

Fig. 18 **a** The variation of the strain energy E_T (normalized by $E_T^{\max} = \pi\mu a^2\epsilon^{\bullet 2}/4$) with b/a, according to (68), where $\epsilon^{\bullet 2} = \epsilon_{zx}^{\bullet 2} + \epsilon_{zy}^{\bullet 2}$. **b** The corresponding variations of $-\partial E_T/\partial b$ and M_C^{incl}/b (normalized by $2\pi\mu a\epsilon^{\bullet 2}$)

The plot of E_T (normalized by $E_T^{\max}$) is shown in Fig. 18a. Of all inclusions of radius $b \le a$, characterized by the same uniform eigenstrain and inserted into a concentric cylinder of radius a, the largest strain energy corresponds to the case $b = a/\sqrt{2}$. The plots of $-\partial E_T/\partial b$ and M_C^{incl}/b are shown in Fig. 18b.

If $(a, d) \to \infty$, while $a - d = c$, (67) gives the expression for the force on the inclusion whose center is at distance c from the free surface of a half-space (Fig. 10). Alternatively, this expression can be obtained from the expression (37) for the shear stress along the free surface, by performing the integration

$$J_x^{\text{incl}} = -\frac{1}{2\mu}\int_{-\infty}^{\infty} \sigma_{zy}^2(0, y)\,\mathrm{d}y = -\pi\mu\,\frac{b^4}{2c^3}\left(\epsilon_{zx}^{\bullet 2} + \epsilon_{zy}^{\bullet 2}\right). \tag{71}$$

The M integral around the inclusion and the energy release rate associated with the expansion of the inclusion in this case are

$$M_C^{\text{incl}} = \pi\mu\,\frac{b^4}{2c^2}\left(\epsilon_{zx}^{\bullet 2} + \epsilon_{zy}^{\bullet 2}\right), \quad -\frac{\partial E_{\mathrm{T}}}{\partial b} = -\pi\mu b\left(2 - \frac{b^2}{c^2}\right)\left(\epsilon_{zx}^{\bullet 2} + \epsilon_{zy}^{\bullet 2}\right), \quad c \ge b, \tag{72}$$

the total strain energy being $E_T = E_T^0[1 - b^2/(4c^2)]$, with $E_T^0 = \pi\mu b^2\left(\epsilon_{zx}^{\bullet 2} + \epsilon_{zy}^{\bullet 2}\right)$.

10 Conclusions

We have derived in this paper the expressions for the stress and displacement fields in an infinite isotropic elastic solid, weakened by a circular cylindrical void, due to a nearby circular inclusion characterized by uniform eigenstrain of the antiplane shear type. The fields are obtained as the sum of their infinite-medium stress fields and the calculated auxiliary fields. The fields outside the inclusion follow directly from the extended Milne–Thomson circle theorem, but not the fields inside the inclusion. It is shown that the overall fields (21)–(24) represent the superposition of the infinite-medium fields of the actual and the image inclusion. If the eigenstrain components of the actual inclusion are $(\epsilon_{zx}^{\bullet}, \epsilon_{zy}^{\bullet})$, the eigenstrain components of the image inclusion are $(\epsilon_{zx}^{*}, \epsilon_{zy}^{*}) = (-\epsilon_{zx}^{\bullet}, \epsilon_{zy}^{\bullet})$. The radius of the image inclusion is $b^* = (a^2/d)b$, where a is the radius of the void, b is the radius of the actual inclusion, and d is the distance between the centers O and C of the void and inclusion. The center of the image inclusion is at the distance $d^* = a^2/d$ from the center of the void. The analysis also delivers the results for the inclusion within a circular cylinder and near the free surface of a half-space. The stress amplification is evaluated for the inclusion approaching the boundary of the void, cylinder, and half-space, being tangent to them in the limiting case.

The second part of the paper is devoted to the determination of configurational forces acting on the void and inclusion. The configurational force associated with a translation of the void is calculated by evaluating the J integral along the boundary of the void, without using the solution of the entire boundary-value problem. This is accomplished by incorporating the result that the circumferential shear stress along the boundary of a circular void in an infinite isotropic elastic solid under antiplane shear is twice the circumferential shear

stress along the corresponding circle in an infinite solid without a void, under the same loading conditions. The configurational force, given by (44), depends on the magnitude of total eigenstrain, but not on the ratio of the eigenstrain components. The force on the inclusion exerted by the void is equal in magnitude and opposite in direction. The maximum value of this force is reached at the minimum distance between the centers of the inclusion and void for which the presented analysis applies, which is when the inclusion is tangent to the void. The interaction energy between the inclusion and void and the total energy (E_T) of the system are then evaluated. The M_O integral around the void is calculated by using only the infinite-medium stress field. The derived expression (56) is shown to be equal to $-a(\partial E_T/\partial a)$, if the surface of the void is traction-free. The M_C integral around the inclusion is given by (59) and is related to the energy release rate $-(\partial E_T/\partial b)$ by (66). The specific configurational force (f) per unit circumference of the boundary of the inclusion is given by (65). The configurational forces on the inclusion in a circular cylinder are evaluated in Sect. 9. If the inclusion of radius b and a prescribed eigenstrain are concentrically inserted in a circular cylinder of radius a, the largest strain energy corresponds to the case $b = a/\sqrt{2}$. The expressions for the J and M integrals for the inclusion near the free surface of a half-space are specified by (71) and (72).

Acknowledgments Research support from the Montenegrin Academy of Sciences and Arts is gratefully acknowledged.

Appendix A: Auxiliary problem by the Fourier series

Since stresses must decay to zero away from the void as $r \to \infty$, the appropriate stress function for the auxiliary problem is

$$\hat{\Psi}(r,\theta) = \mu\hat{w}(r,\theta) = \sum_{n=1}^{\infty} \frac{1}{r^n}\left(\hat{A}_n \cos n\theta + \hat{B}_n \sin n\theta\right). \tag{A.1}$$

The corresponding radial shear stress is

$$\hat{\sigma}_{zr}(r,\theta) = \frac{\partial\hat{\Psi}}{\partial r} = -\sum_{n=1}^{\infty} \frac{n}{r^{n+1}}\left(\hat{A}_n \cos n\theta + \hat{B}_n \sin n\theta\right). \tag{A.2}$$

The constants $\hat{A}_n$ and $\hat{B}_n$ are specified by imposing the boundary condition $\hat{\sigma}_{zr}(a,\theta) = -\sigma^0_{zr}(a,\theta)$, where $\sigma^0_{zr}(a,\theta)$ is, from (5), given by

$$\sigma^0_{zr}(a,\theta) = -\frac{\mu b^2}{\rho_a^4}\left\{\left[(d^2+a^2)\cos\theta - 2da\right]\epsilon^{\bullet}_{zx} - \left[(d^2-a^2)\sin\theta\right]\epsilon^{\bullet}_{zy}\right\}. \tag{A.3}$$

Here, $\rho_a^2 = d^2 - 2da\cos\theta + a^2$ is the square of the distance from the center of the inclusion to an arbitrary point on the boundary of the void (Fig. 1a). By applying the Fourier series analysis, there follows

$$\hat{A}_n = -\frac{\mu b^2}{d} d_*^n \epsilon^{\bullet}_{zx}, \quad \hat{B}_n = \frac{\mu b^2}{d} d_*^n \epsilon^{\bullet}_{zy}, \tag{A.4}$$

with $d_* = a^2/d$. Thus, by substituting (A.4) into (A.1), the stress function of the auxiliary problem becomes

$$\hat{\Psi}(r,\theta) = -\frac{\mu b^2}{d}\sum_{n=1}^{\infty} \frac{1}{(r/d_*)^n}\left(\epsilon^{\bullet}_{zx}\cos n\theta - \epsilon^{\bullet}_{zy}\sin n\theta\right). \tag{A.5}$$

Recalling the Laurent series of the function of the complex variable $z = (r/d_*)e^{i\theta}$ [49],

$$\frac{1}{1-z} = -\sum_{n=1}^{\infty}\frac{1}{z^n}, \quad |z| > 1, \tag{A.6}$$

by taking the real and imaginary parts of (A.6) it follows that

$$\sum_{n=1}^{\infty} \frac{\cos n\theta}{(r/d_*)^n} = \frac{(r/d_*)\cos\theta - 1}{1 - 2(r/d_*)\cos\theta + (r/d_*)^2},$$
$$\sum_{n=1}^{\infty} \frac{\sin n\theta}{(r/d_*)^n} = \frac{(r/d_*)\sin\theta}{1 - 2(r/d_*)\cos\theta + (r/d_*)^2}. \tag{A.7}$$

Upon substitution of (A.7) into (A.5), the stress function takes the form

$$\hat{\Psi}(r,\theta) = \frac{\mu b_*^2}{\rho_*^2}\left[(r\cos\theta - d_*)\epsilon_{zx}^* + (r\sin\theta)\epsilon_{zy}^*\right], \tag{A.8}$$

where $b_* = ab/d$, $\left(\epsilon_{zx}^*, \epsilon_{zy}^*\right) = \left(-\epsilon_{zx}^\bullet, \epsilon_{zy}^\bullet\right)$, and $\rho_*^2 = d_*^2 - 2d_* r\cos\theta + r^2$. The corresponding displacement is $\hat{w} = \hat{\Psi}/\mu$, while the stress components are $\hat{\sigma}_{zr}(r,\theta) = \partial\hat{\Psi}/\partial r$ and $\hat{\sigma}_{z\theta}(r,\theta) = r^{-1}\partial\hat{\Psi}/\partial\theta$, which reproduces (17) and (20). In particular, $\hat{\sigma}_{z\theta}(a,\theta) = \sigma_{z\theta}^0(a,\theta)$.

Appendix B: Integrals used to evaluate J and M integrals

The following integrals were used in the derivation of the J and M integrals in Sects. 7 and 8:

$$I_1 = \int_0^\pi \frac{\sin^2\theta\cos\theta\,\mathrm{d}\theta}{\rho^8} = \frac{\pi}{a^8}\frac{d/a}{[(d/a)^2-1]^5} = I_2 - I_4,$$
$$I_2 = \int_0^\pi \frac{\cos\theta\,\mathrm{d}\theta}{\rho^8} = \frac{4\pi}{a^8}\frac{d/a}{[(d/a)^2-1]^7}\left[\left(\frac{d^2}{a^2}+1\right)^2 + \frac{d^2}{a^2}\right],$$
$$I_3 = \int_0^\pi \frac{\cos^2\theta\,\mathrm{d}\theta}{\rho^8} = \frac{\pi}{2a^8}\frac{(d/a)^2+1}{[(d/a)^2-1]^7}\left[\left(\frac{d^2}{a^2}+1\right)^2 + 16\frac{d^2}{a^2}\right],$$
$$I_4 = \int_0^\pi \frac{\cos^3\theta\,\mathrm{d}\theta}{\rho^8} = \frac{\pi}{a^8}\frac{d/a}{[(d/a)^2-1]^7}\left[3\left(\frac{d^2}{a^2}+1\right)^2 + 8\frac{d^2}{a^2}\right],$$
$$I_5 = \int_0^\pi \frac{\sin^2\theta\,\mathrm{d}\theta}{\rho^8} = \frac{\pi}{2a^8}\frac{(d/a)^2+1}{[(d/a)^2-1]^5} = I_6 - I_3,$$
$$I_6 = \int_0^\pi \frac{\mathrm{d}\theta}{\rho^8} = \frac{\pi}{a^8}\frac{(d/a)^2+1}{[(d/a)^2-1]^7}\left[\left(\frac{d^2}{a^2}+1\right)^2 + 6\frac{d^2}{a^2}\right]$$

where $\rho^2 = d^2 - 2ad\cos\theta + a^2$. These expressions were derived by using the formulas listed in [50], pages 148–149, in conjunction with appropriate integration by parts. The expressions were also verified by Matlab evaluation of integrals.

The integrals used in the evaluation of the Fourier coefficients of the auxiliary problem are:

$$\int_0^\pi \frac{\sin\theta\sin n\theta\,\mathrm{d}\theta}{\rho^2} = \frac{\pi}{2a^2}\left(\frac{a}{d}\right)^{n+1}, \quad n \geq 1,$$
$$\int_0^\pi \frac{\cos\theta\cos n\theta\,\mathrm{d}\theta}{\rho^2} = \frac{\pi}{2a^2}\frac{d^2+a^2}{d^2-a^2}\left(\frac{a}{d}\right)^{n+1},$$
$$\int_0^\pi \frac{\sin\theta\sin n\theta\,\mathrm{d}\theta}{\rho^4} = \frac{n\pi}{2ad}\frac{(a/d)^n}{d^2-a^2},$$
$$\int_0^\pi \frac{\cos\theta\cos n\theta\,\mathrm{d}\theta}{\rho^4} = \frac{\pi}{2ad}\frac{(a/d)^n}{(d^2-a^2)^3}[4a^2d^2 + n(d^4-a^4)].$$

References

1. Yang, H.C., Chou, Y.T.: Antiplane strain problems of an elliptical inclusion in an anisotropic medium. J. Appl. Mech. **44**, 437–441 (1977)
2. Masumura, R.A., Chou, Y.T.: Antiplane eigenstrain problem of an elliptic inclusion in an anisotropic half space. J. Appl. Mech. **49**, 52–54 (1982)
3. Zhang, H.T., Chou, Y.T.: Antiplane eigenstrain problem of an elliptic inclusion in a two-phase anisotropic medium. J. Appl. Mech. **52**, 87–90 (1985)
4. Ru, C.Q.: Eshelby inclusion of arbitrary shape in an anisotropic plane or half-plane. Acta Mech. **160**, 219–234 (2003)
5. Wang, R.: Antiplane eigenstrain problem of a circular inclusion in nonlocal elasticity. Acta Mech. **85**, 131–136 (1990)
6. Lubarda, V.A.: Circular inclusions in anti-plane strain couple stress elasticity. Int. J. Solids Struct. **40**, 3827–3851 (2003)
7. Haftbaradaran, H., Shodja, H.M.: Elliptic inhomogeneities and inclusions in anti-plane couple stress elasticity with application to nano-composites. Int. J. Solids Struct. **46**, 2978–2987 (2009)
8. Pak, Y.E.: Circular inclusion problem in antiplane piezoelectricity. Int. J. Solids Struct. **29**, 2403–2419 (1992)
9. Honein, T., Honein, B.V., Honein, E., Herrmann, G.: On the interaction of two piezoelectric fibers embedded in an intelligent material. J. Intell. Mater. Syst. Struct. **6**, 229–236 (1995)
10. Xiao, Z.M., Yan, J., Chen, B.J.: Electro-elastic stress analysis for a screw dislocation interacting with a coated inclusion in piezoelectric solid. Acta Mech. **172**, 237–249 (2004)
11. Wang, X., Pan, E., Roy, A.K.: A functionally graded plane with a circular inclusion under uniform antiplane eigenstrain. J. Appl. Mech. **75**, 014501-1–014501-4 (2008)
12. Yavari, A., Goriely, A.: Nonlinear elastic inclusions in isotropic solids. Proc. R. Soc. Lond. A **469**, Art. 20130415 (2013)
13. Honein, E., Honein, T., Herrmann, G.: On two circular inclusions in harmonic problems. Q. Appl. Math. **50**, 479–499 (1992)
14. Honein, E., Honein, T., Herrmann, G.: Further aspects on the elastic field for two circular inclusions in antiplane elastostatics. J. Appl. Mech. **59**, 774–779 (1992)
15. Ru, C.Q., Schiavone, P.: A circular inclusion with circumferentially inhomogeneous interface in antiplane shear. Proc. R. Soc. Lond. A **453**, 2551–2572 (1997)
16. Wang, X., Shen, Y.-P.: Two circular inclusions with inhomogeneous interfaces interacting with a circular Eshelby inclusion in anti-plane shear. Acta Mech. **158**, 67–84 (2002)
17. Friedel, J.: Dislocations. Pergamon Press, Reading, MA (1964)
18. Dundurs, J., Mura, T.: Interaction between an edge dislocation and a circular inclusion. J. Mech. Phys. Solids **12**, 177–189 (1964)
19. Dundurs, J.: Elastic interactions of dislocations with inhomogeneities. In: Mura, T. (ed.) Mathematical Theory of Dislocations, pp. 70–115. ASME, New York (1969)
20. Eshelby, J.D.: Boundary problems. In: Nabarro, F.R.N. (ed.) Dislocations in Solids, vol. 1, pp. 167–221. North Holland, Amsterdam (1979)
21. Lubarda, V.A., Schneider, M.S., Kalantar, D.H., Remington, B.R., Meyers, M.A.: Void growth by dislocation emission. Acta Mater. **52**, 1397–1408 (2004)
22. Meyers, M.A., Traiviratana, S., Lubarda, V.A., Bringa, E.M., Benson, D.J.: The role of dislocations in the growth of nanosized voids in ductile failure of metals. J. Mater. **61**, 35–41 (2009)
23. Rudd, R.E.: Void growth in bcc metals simulated with molecular dynamics using the Fennis–Sinclair potential. Philos. Mag. **89**, 3133–3161 (2009)
24. Lubarda, V.A.: Image force on a straight dislocation emitted from a cylindrical void. Int. J. Solids Struct. **48**, 648–660 (2011)
25. Lubarda, V.A.: Emission of dislocations from nanovoids under combined loading. Int. J. Plast. **27**, 181–200 (2011)
26. Gong, S.X.: A unified treatment of the elastic elliptical inclusion under antiplane shear. Arch. Appl. Mech. **65**, 55–64 (1995)
27. Chen, Y.Z.: Image method for curved crack problem in antiplane elasticity. Int. J. Fract. **48**, R75–R78 (1991)
28. Zhou, K., Hoh, H.J., Wang, X., Keer, L.M., Pang, J.H.L., Song, B., Wang, Q.J.: A review of recent works on inclusions. Mech. Mater. **60**, 144–158 (2013)
29. Milne-Thomson, L.M.: Hydrodynamical images. Proc. Camb. Philos. Soc. **36**, 246–247 (1940)
30. Milne-Thomson, L.M. : Theoretical Hydrodynamics. Macmillan Press, London (1968)
31. Smith, E.: The interaction between dislocations and inhomogeneities – I. Int. J. Eng. Sci. **6**, 129–143 (1968)
32. Lin, W.-W., Honein, T., Herrmann, G.: A novel method of stress analysis of elastic materials with damage zones. In: Boehler, J.P. (ed.), Yielding, Damage, and Failure of Anisotropic Solids, EGF Publication 5, pp. 609–615. Mechanical Engineering Publications, London (1990)
33. Hirth, J.P., Lothe, J.: Theory of Dislocations. 2nd edn. Wiley, New York (1982)
34. Mura, T.: Micromechanics of Defects in Solids. 2nd edn. Kluwer Academic Publishers, Dordrecht (1987)
35. Barber, J.R.: Elasticity–Solid Mechanics and its Applications. 3rd edn. Springer, New York (2010)
36. Eshelby, J.D.: The calculation of energy release rates. In: Sig, G.C. (ed.) Prospects of Fracture Mechanics, pp. 69–84. Noordhoff, Leyden, The Netherlands (1975)
37. Freund, L.B.: Stress intensity factor calculations based on a conservation integral. Int. J. Solids Struct. **14**, 241–250 (1978)
38. Rice, J.R.: Conserved integrals and energetic forces. In: Bilby, B.A., Miller, K.J., Willis, J.R. (eds.) Fundamentals of Deformation and Fracture, pp. 33–56. Cambridge University Press, Cambridge (1985)
39. Kienzler, R., Kordisch, H.: Calculation of J_1 and J_2 using the L and M integrals. Int. J. Fract. **43**, 213–225 (1990)
40. Müller, W.H., Kemmer, G.: Applications of the concept of J-integrals for calculation of generalized forces. Acta Mech. **129**, 1–12 (1998)
41. Honein, E., Honein, T., Herrmann, G.: Energetics of two circular inclusions in anti-plane elastostatics. Int. J. Solids Struct. **37**, 3667–3679 (2000)
42. Lubarda, V.A.: On the non-uniqueness of solution for screw dislocation in multiply connected regions. J. Elast. **52**, 289–292 (1999)

43. Lubarda, V.A., Markenscoff, X.: The stress field for a screw dislocation near cavities and straight boundaries. Mater. Sci. Eng. A **349**, 327–334 (2003)
44. Kienzler, R., Zhuping, D.: On the distribution of hoop stresses around circular holes in elastic sheets. J. Appl. Mech. **54**, 110–114 (1987)
45. Eshelby, J.D.: The continuum theory of lattice defects. Solid State Phys. **3**, 79–144 (1956)
46. Knowles, J.K., Sternberg, E.: On a class of conservation laws in linearized and finite elastostatics. Arch. Ration. Mech. Anal. **44**, 187–211 (1972)
47. Budiansky, B., Rice, J.R.: Conservation laws and energy-release rates. J. Appl. Mech. **40**, 201–203 (1973)
48. Gavazza, S.D.: Forces on pure inclusions and Somigliana dislocations. Scr. Metall. **11**, 977–981 (1977)
49. Muskhelishvili, N.I.: Some Basic Problems of the Mathematical Theory of Elasticity. P. Noordhoff, Groningen (1953)
50. Gradshteyn, I.S., Ruzhik, I.W.: Tables of Integrals, Sums and Products (corrected and enlarged edition). Academic Press, New York (1965)